Perspectives for SPH Applications on Shock Wave Problems: Basic Modeling and Preliminary Tests

Roberto Guandalini[*1], Giordano Agate[*1], Sauro Manenti[2], Stefano Sibilla[2], Mario Gallati[2]

[1] RSE s.p.a. Environment and Sustainable Development Dept., Via Rubattino, 54 – 20134 Milan, Italy

[2] University of Pavia, Dept. Of Hydraulic and Environmental Eng. via Ferrata, 1 27100 Pavia Italy

[*1]giordano.agate@rse-web.it; roberto.guandalini@rse-web.it;
[2]sauro.manenti@unipv.it; stefano.sibilla@unipv.it; gallati@unipv.it

Abstract

The paper shows an application of the Smoothed Particle Hydrodynamics (SPH) for the numerical modeling of engineering problems involving rapid evolution over time as large strains and gradients, heterogeneity, deformable contours, mobile material interfaces and free surfaces.

Following a Lagrangian approach, the continuum is discretized by means of a finite number of material particles carrying physical properties and moving according to Newton's equations of the classical physics. Spatial derivatives of a variable at a point are approximated by using the information on the neighboring particles based on the kernel approximation.

The paper provides a brief description of the basics of the method along with some numerical aspects concerning boundary treatment and time integration scheme. Furthermore, some more details are provided about the recent improvements achieved with the aim of performing future SPH simulations involving underwater explosion for bottom sediment resuspension and flushing in an artificial reservoir.

Numerical examples are illustrated and discussed concerning the early 2D test cases investigating the basic features of gas explosion; and obtained results show thateven if some improvements are required to overcome the model limitations, the SPH method is promising to reproduce the impulsive dynamics of the underwater sediments. Besides that, a feasibility study has been scheduled in order to investigate possible applications in innovative fields as the Enhanced Geothermal Systems for geothermal energy production.

Keywords

Smoothed Particle Hydrodynamics; Underwater Explosion; Multiphase Analisys

Introduction

The core idea of a meshfree method is to obtain a discretization of the continuum through a set of arbitrarily distributed nodes (or particles) that are lack of a connective mesh and can be adapted to possible topological and geometrical changes.

With respect to traditional grid-based approaches, a meshless method allows tracing the deformation undergone by the material without excessive degradation of numerical results (owing to conflicts between mesh and physical compatibility) and high computational effort (e.g. adaptive mesh refinement).

When the nodes assume a physical meaning (i.e. they represent material particles carrying physical properties such as mass, momentum etc.) the method is said a meshfree particle method and follows, in general, a Lagrangian approach.

Among the different meshfree particle methods, the Smoothed Particle Hydrodynamics (SPH) was originally developed as a probabilistic model to simulate astrophysical problems [Lucy, Gingold & Monaghan], and later modified as a deterministic meshfree particle method and applied to continuum solid and fluid mechanics [Monaghan 1992, Monaghan 1992a] because the kinematics and dynamics of the liquid particles, responding to Newton's equations of the classical physics, could be described in analogy with the simulation of the collective movement of astrophysical particles at large scale.

According to standard SPH, a continuous physical quantity $A(x)$, defined on the spatial domain Ω as a function of the position vector x, and its spatial derivatives at the i–th material point, is approximated by using the information on the neighboring particles based on the kernel estimate.

This procedure adopts a kernel function $W(r, h)$, which is continuous, non-zero and depends on the modulus

of the relative position $r = |\boldsymbol{x}_i - \boldsymbol{x}_j|$ of the neighboring j–th particle falling within a circular space (spherical in 3D problems) with radius $2h$, where h is generally referred to as the smoothing length (Fig.1).

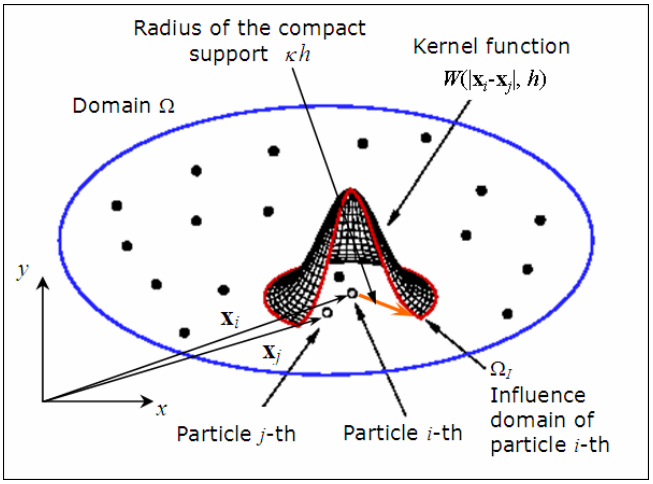

FIG. 1 TYPICAL REPRESENTATION OF PARTICLE DISCRETIZATION AND KERNEL FUNCTION

The SPH approximation of the field function $A(x)$ originates from the concept of integral representation:

$$A(\mathbf{x}) = \int_{\Omega} \delta(\mathbf{x}-\mathbf{x}')\, A(\mathbf{x}')\, d\Omega_{x'} \tag{1}$$

In Eq.1, the Dirac delta function δ is replaced by the kernel function leading to the kernel approximation:

$$\langle A(\mathbf{x})\rangle = \int_{\Omega} W(r,h) A(\mathbf{x}')\, d\Omega_{\mathbf{x}'} \tag{2}$$

Considering the set of material particles representing the discretized continuum, the discrete form of the Eq.2 is obtained through the so called particle approximation that leads to the estimate of the field function A at the i-th particle:

$$\langle A(\mathbf{x}_i)\rangle = \sum_{j=1}^{N} \frac{m_j}{\rho_j} A(\mathbf{x}_j) W(r_{ij}, h) \tag{3}$$

The summation in Eq.3 is extended over the N–neighboring particles, having volume $\Delta V_j = m_j/\rho_j$, falling within the compact support (or influence domain) Ω_I of the i–th particle.

In a similar fashion, it can be demonstrated that the particle approximation of the function derivative can be obtained by shifting the differential operator on the kernel; and two alternative expressions are commonly adopted in fluid mechanics [Li & Liu, 2004]:

$$\begin{aligned} \langle \nabla \cdot A(\mathbf{x}_i)\rangle &= \frac{1}{\rho_i}\sum_{j=1}^{N} m_j \left[A(\mathbf{x}_j) - A(\mathbf{x}_i)\right] \cdot \nabla W(r_{ij}, h) \\ \langle \nabla \cdot A(\mathbf{x}_i)\rangle &= \rho_i \sum_{j=1}^{N} m_j \left[\frac{A(\mathbf{x}_j)}{\rho_j^2} + \frac{A(\mathbf{x}_i)}{\rho_i^2}\right] \cdot \nabla W(r_{ij}, h) \end{aligned} \tag{4}$$

By applying the SPH interpolation, the Lagrangian form of the Navier-Stokes equations for a weakly compressible viscous fluid can be transformed into a system of ordinary differential equations that, by adopting the equations (4) and replacing $W(r_{ij}, h)$ with Wij, are written as:

$$\begin{aligned} \left\langle \frac{D\rho}{Dt} \right\rangle_i &= -\sum_{j=1}^{N} m_j (\mathbf{u}_j - \mathbf{u}_i) \cdot \nabla W_{ij} \\ \left\langle \frac{D\mathbf{u}}{Dt} \right\rangle_i &= -\sum_{j=1}^{N} m_j \left(\frac{p_i}{\rho_i^2} + \frac{p_j}{\rho_j^2} + \Pi_{ij}\right) \nabla W_{ij} + \mathbf{g} \\ &\quad + \sum_{j=1}^{Ni} \frac{m_j}{\rho_i \rho_j} \frac{4\mu_i \mu_j}{\mu_i + \mu_j} \frac{\mathbf{x}_{ij} \cdot \nabla W_{ij}}{\mathbf{x}_{ij}^2 + 0.01h^2} \mathbf{u}_{ij} \end{aligned} \tag{5}$$

The additional term Π_{ij} in Eq.5 is the so called Monaghan artificial viscosity [Monaghan 1992a] often introduced instead of the physical viscosity for numeric stability:

$$\Pi_{ij} = \begin{cases} \dfrac{-\alpha_M (c_{si} + c_{sj})}{\rho_i + \rho_j} \varphi_{ij} + \dfrac{2\beta_M}{\rho_i + \rho_j} \varphi_{ij}^2 & \text{if } \mathbf{u}_{ij} \cdot \mathbf{x}_{ij} < 0 \\ 0 & \text{if } \mathbf{u}_{ij} \cdot \mathbf{x}_{ij} > 0 \end{cases} \tag{6}$$

$$\varphi_{ij} = \frac{h\, \mathbf{u}_{ij} \cdot \mathbf{x}_{ij}}{\mathbf{x}_{ij}^2 + (0.1h)^2}$$

There are several advantages that can be obtained from such an approach: representation of the evolution of both free-surfaces, moving-interfaces and breaking waves, becomes more simple to face [Manenti 2008]; treatment of large deformation and shock problems becomes a relatively easier task [Di Monaco]; the particle tracking along with the relevant field variables can be obtained by numerical solution of the discretized set of governing equations in Lagrangian form [Manenti 2011].

Numerical Aspects

The solution strategy of a meshfree particle method follows a pattern similar to a grid-based method.

The computational domain is divided into a finite number of particles, followed by the numerical discretization of the system of partial differential equations according to the procedure described in the previous section and the resulting ordinary differential equations are solved through any stable time-stepping algorithm [Monaghan 2005]: here a first order explicit numerical scheme is used and a cubic spline function is adopted for kernel representation [Di Monaco].

The obtained velocity field allows one to update the particle position x and to compute the density field by means of the continuity equation (1); the pressure p_i at each point is generally calculated through the equation

of state for a weakly compressible fluid and then smoothed out:

$$p_i = p_{0i} + \frac{\varepsilon}{\rho}\left(\rho_i - \rho_{0i}\right)$$
$$p_i^{smth} = p_i + \vartheta_p \frac{\sum_{j=1}^{N}\left(p_j - p_i\right)\Delta V_j W_{ij}}{\sum_{j=1}^{N}\Delta V_j W_{ij}} \quad (7)$$

Solid boundaries are treated by means of the semi-analytic technique [Di Monaco]. Each portion of the solid contour, contributing to the mass and momentum equations of the generic *i*-th particle, is replaced by a fluid region extending beyond the boundary and treated as a material continuum with uniform velocity ($\boldsymbol{u}_b = \boldsymbol{u}_i$), and hydrostatic pressure distribution (Fig.2).

A typical term for boundary contribution in the balance equations is:

$$C_1 \int_\alpha C_2 \; J_n(\vartheta,\phi)\, d\alpha$$
$$\text{with:} \quad C_1 = f(\rho_i, \mathbf{u}_i, \mathbf{u}_b, \nu) \quad (8)$$
$$C_2 = f(\nabla r) \qquad J_n(\vartheta,\phi) = \int_{r_b(\vartheta,\phi)}^{2h} \frac{dW}{dr} r^n dr$$

In Eq.8 $\alpha = f(\vartheta, \varphi)$ denotes the solid angle under which the *i*-th particle sees the portion of the solid boundary intersected by its sphere of influence and the integrals J_n (n=1, 2, 3) depends on the boundary's geometry and can be computed analytically.

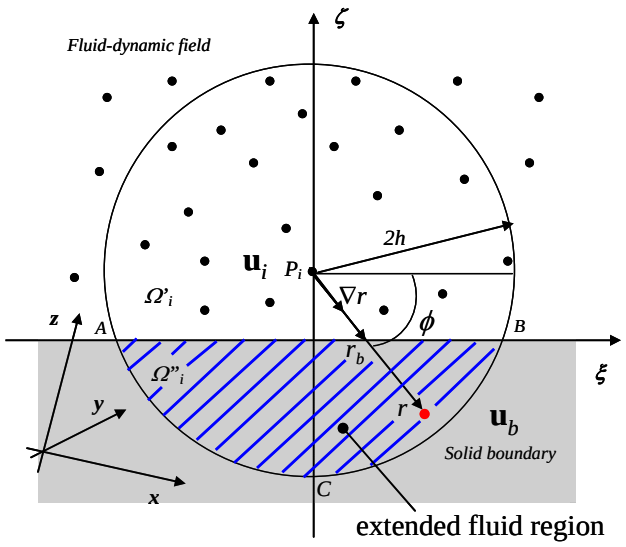

FIG. 2 SKETCH OF SOLID BOUNDARY TREATMENT (2D CASE).

Modeling Gas Explosion

The explosion process of a high explosive (HE) material is characterized by a violent oxidation involving a chemical compound and an oxidizer; since the internal energy of the products is lower than the one of the reactants, a large amount of heat (say reaction heat) is quickly released [Cooper].

Even if such a phenomenon develops at very high speed of reaction, in the early phase it is characterized by two distinct inhomogeneous zones: a detonation-produced explosive gas and a non-oxidized explosive, between which a very thin layer exists representing the front of a reacting shock wave (detonation wave) advancing with a characteristic velocity **U**.

Anyway, in several applications, the detonation speed can be assumed indefinitely high and the HE charge completely transformed into gaseous products whose expansion can be analyzed by considering the Euler equation for an inviscid fluid and assuming adiabatic process [Manenti 2008, Morris].

As a result, the viscous contribution at the right hand side of the linear momentum Eq.5 is neglected, and a balance equation for the gas internal energy is introduced:

$$\left\langle \frac{De}{Dt} \right\rangle_i = \frac{1}{2}\sum_{j=1}^{N} m_j \left(\frac{p_i}{\rho_i^2} + \frac{p_j}{\rho_j^2} + \Pi_{ij} \right)\left(\mathbf{u}_i - \mathbf{u}_j\right)\cdot \nabla W_{ij} \quad (14)$$

The state equation given by eq.15 is used for adiabatic transformation.

$$p_i = \left(\gamma - 1\right)\rho_i e_i \qquad c_s^2 = \gamma\left(\gamma - 1\right) e = \frac{\varepsilon}{\rho_i} \quad (15)$$

The kernel function adopted in subsequent analyses is a cubic spline, while the time integration is carried out through an explicit numerical scheme derived from the symplectic algorithm [Manenti 2010].

Numerical Examples

This section illustrates the numerical results concerning two basic 2D SPH simulations of gas explosion: in the first of which a circular charge surrounded by a water crown expands inside a squared box with rigid walls; while in the other a squared charge expands inside an underwater sediment layer. The numerical model previously described is adopted.

Gas Explosion

In the following, the numerical results are shown concerning the expansion process of a HE detonated gas and the circular charge in vacuum is firstly considered (see Fig. 3); subsequently the charge is surrounded by a water crown (see Fig. 4) while in both cases the process is confined within a rigid box. As previously reported, the modulus of the detonation velocity U is assumed to be indefinitely high with respect to the gas kinematic, thus the explosive charge

is assumed completely detonated.

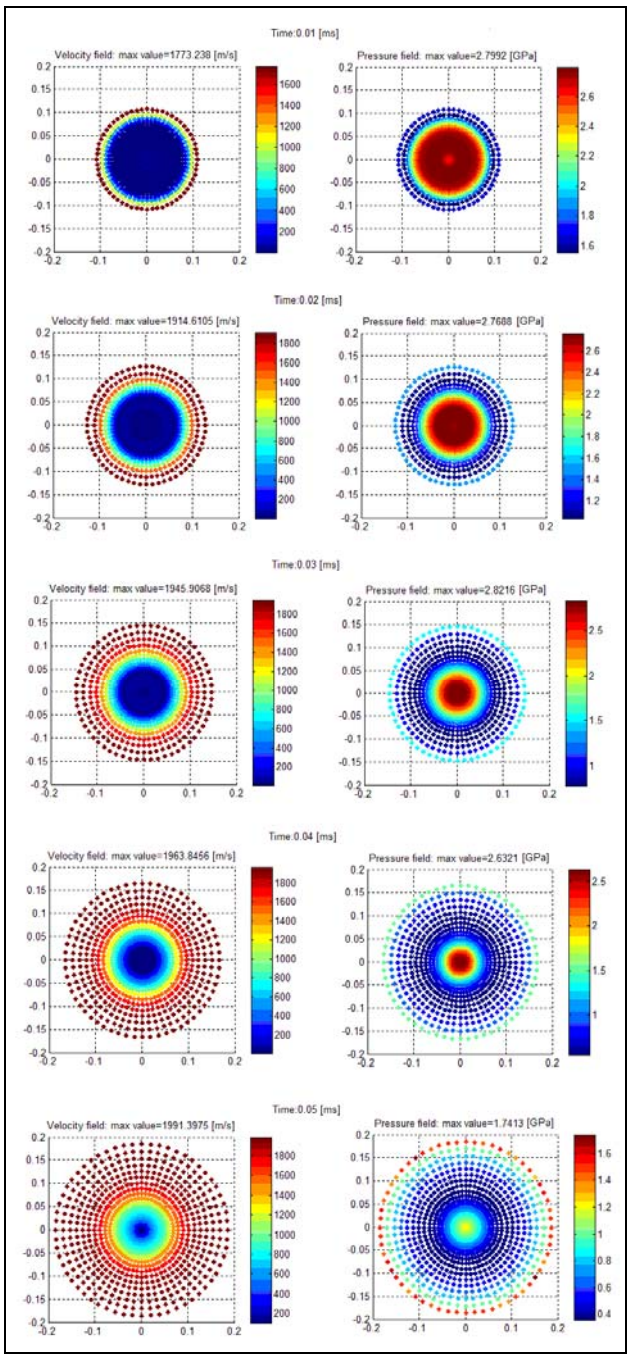

FIG. 3 EXPANSION OF DETONATED GAS IN VACUUM INSIDE A RIGID BOX; AXES SCALE IN METERS

Table 1 summarizes the relevant model parameters adopted in subsequent computations.

When considering the vacuum gas expansion, at the initial time, 20 particles are placed in the radial direction while 60 particles are positioned along the tangential direction at the external boundary, resulting in a total number of 1200. The particle position, velocity (modulus) and pressure are depicted in Fig. 3 at time intervals of 10 μs and axes labels are in meters.

The charge centre represents a singular point since no particle is placed on it and this explains the lower pressure.

The expansion process reflects theoretical expectation until t = 40 μs: past that time some irregularities in the pressure distribution at the outer boundary of the gaseous mass appear; therefore such a fact should be connected with the lack of information owing to the small number of neighbors in the interaction domain of external particles.

TABLE 1 PRINCIPAL MODEL PARAMETERS ADOPTED FOR GAS EXPLOSION COMPUTATIONS

MODEL PARAMETERS			
η_0	interparticles distance	0.005	m
η	smoothing length	1.3 h_0	m
ρ_0	water ref. density	1000	kg/m³
ρ^{γ}_0	gas ref. density	1630	kg/m³
ε_0	spec. detonation energy	4.29E+06	J/kg
χ_σ	speed of sound	5.0E+04	m/s
α_M	artificial viscosity param.	0.2	-
β_M	artificial viscosity param.	10.0	-
ϑ_ϖ	velocity smoothing	0.2	-
γ_Ω	water state equation param.	1.4 – 7.0	-
γ_Γ	gas state equation param.	1.4	-

Such non-physical behavior is however avoided if a surrounding medium is considered for confinement of the explosive charge, as illustrated in the following.

Fig. 4 shows the expansion of a circular charge surrounded by a water crown and confined in a rigid squared box with length of 0.30 m and the simulation is carried out considering the same value of the state equation parameter for both gas and water (i.e. $\gamma_G / \gamma_W = 1$, see Tab. 1).

The upper left-hand panel displays the initial configuration and the position of the gauges for pressure detection on the transversal and diagonal directions and continuous green line denotes the rigid box walls. The central and the right-hand upper panels show particles position, velocity modulus and pressure at time t = 0.07 ms when the water impacts against the box walls.

The lower panel shows pressure distribution at initial time (t=0.0ms) and at the impact time (t=0.07ms): in the latter a pressure wave is reflected by the box wall and propagates backward along the transversal direction with a pressure peak of about 1 GPa.

The simulation ends at 0.2ms: after the gas and water particles have completely expand occupying the whole box internal volume. In addition, symmetrical jets originate from both transversal and diagonal directions thus pumping the gas toward the box center and producing a contraction of its volume (not

displayed in Fig. 4).

Fig. 5 shows the results obtained when the value of the gamma water constant in the state equation (i.e. γ_G / γ_W = 0.2) is increased to 7.0.

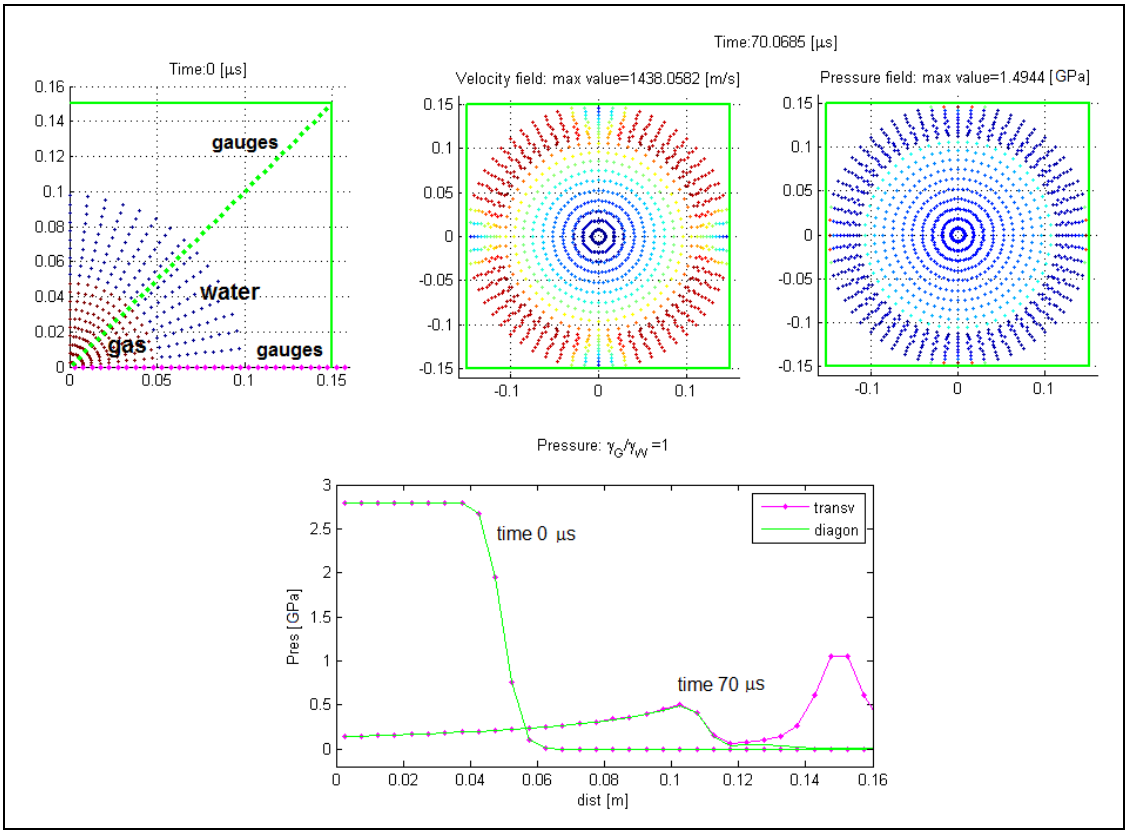

FIG. 4 EXPANSION OF DETONATED GAS SURROUNDED BY A WATER CROWN INTO A RIGID BOX; AXES SCALE IN METERS (γ_G/γ_W = 1)

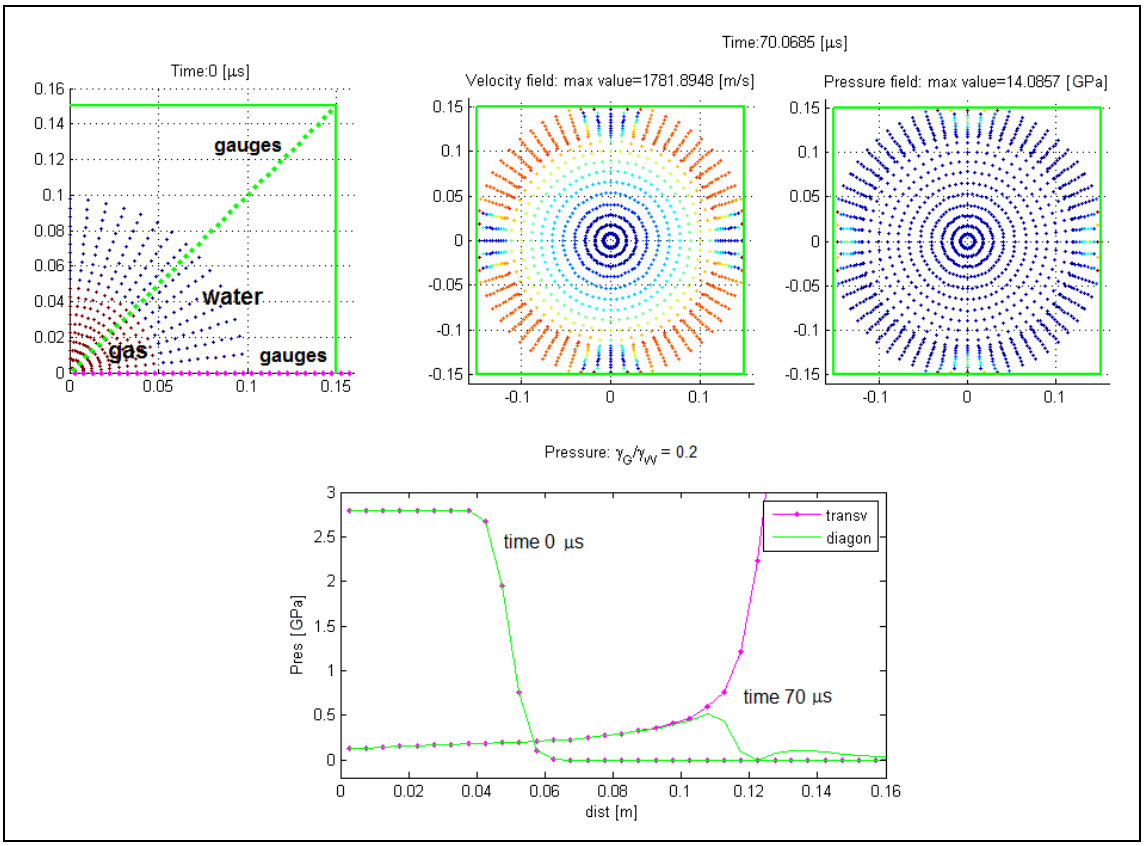

FIG. 5 EXPANSION OF DETONATED GAS SURROUNDED BY A WATER CROWN INTO A RIGID BOX; AXES SCALE IN METERS (γ_G/γ_W=0.2)

The particles dynamics is rather similar to that one described in the case γ_G / γ_W = 1: anyway as now the water compressibility modulus is greater than the gas and this produces reflected pressure waves with higher peaks and celerity.The pulsation frequency of the gas expansion-contraction cycle is increased with respect to the case with γ_G / γ_W = 1.

Underwater Explosion Inside non-Cohesive Sediment

In this numerical test, a squared HE charge is placed below the surface of a sediment layer at the bottom of a water tank, which represents a first attempt toward the investigation of a multiphase shock problem that becomes important in the development of an alternative methodology for siltation control in an artificial reservoir by means of combined use of explosive charges and a flushing manoeuvre (Manenti, 2012).

The principal parameters for the considered materials are summarized in Table 2. The adopted value of the sound speed has been calculated through the last equation in (15) assuming the gamma constant γ_G and the initial specific internal energy e_0 of the HE explosive. The compressibility modulus of each medium has been determined by assuming c_s=155 m/s and the density of the corresponding material. During the expansion, the water-sediment mixture has been simulated as first approximation, like a viscous fluid and this assumption appears reasonable based on the rapid increase of the pore water pressure in the solid matrix around the explosive charge, as discussed in the following.

TABLE 2 MODEL PARAMETERS FOR WATER-GAS EXPLOSION COMPUTATIONS

MODEL PARAMETERS			
	Water	**Sediment**	**HE explosive**
ρ [kg/m^3]	1000.0	1750.0	1630.0
μ [Pa s]	0.0	0.0	0.0
γ [-]	2.4	2.4	1.4
e_0 [J/kg]	252.0	145.0	4.29e+06
h [m]	0.06	0.06	0.06
c_S [m/s]	155.0	155.0	155.0
α_M [-]	2.0	2.2	1.0
θ [-]	0.2	0.2	0.2

Figure 6 shows the obtained results. The upper panel displays the initial configuration and the distribution of the materials. The frame at t=260 μs shows the shock wave propagation after the HE gas expansion, additionally, the initial value of e_0=4.29e+05 J/kg for the specific internal energy has been assumed.

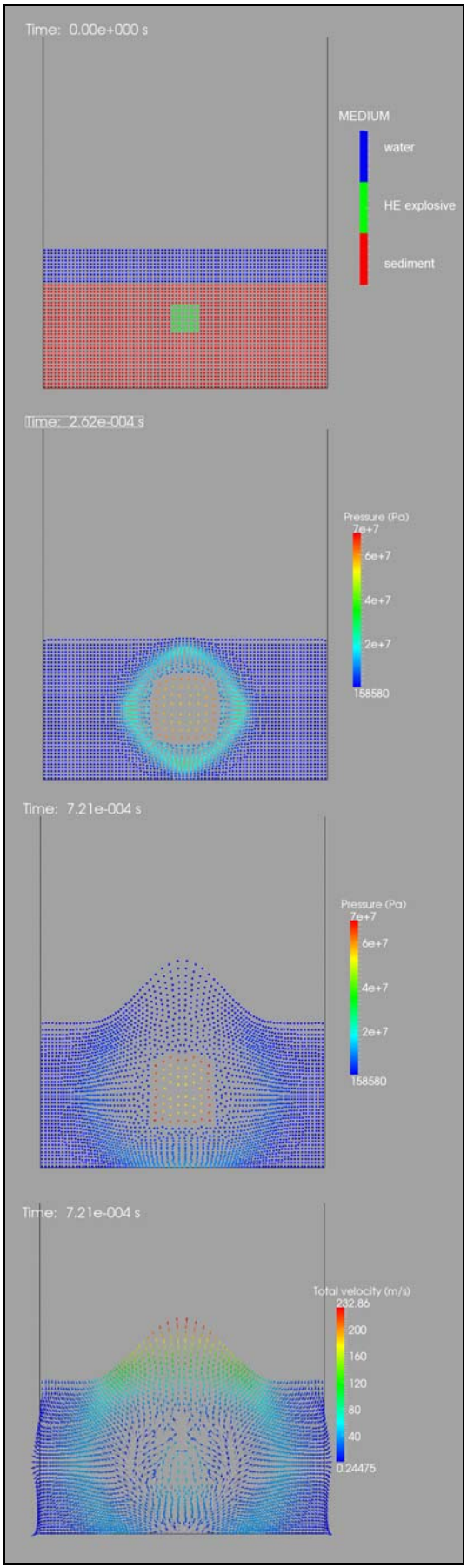

FIG. 6 UNDERWATER EXPLOSION IN A NON-COHESIVE SEDIMENT DEPOSIT

The frame at t = 720 μs shows the formation of a typical pinnacle just above the charge, and the pressure inside the sediment and water layers falls to values around 0.5 MPa and great part of the initial internal energy is transformed into kinetic energy, as illustrated in the lower panel showing the distribution of the velocity modulus and direction.

Experimental investigations should be carried out in order to provide a data base to validate the SPH code; anyway the obtained results seem to be quite acceptable from a qualitative point of view and be in agreement with theoretical expectations.

Note that there are several zones of the domain that are characterized by a coarse particle resolution, especially in the rarefied gaseous mass, which could cause the reduction of neighbours to very low values thus lowering the accuracy of the numerical computation.

A particle refinement technique, such as that one proposed in [Liu] could be helpful for solving the above problem.

Application Perspectives in Geophysics

The advanced SPH applications previously described have been focused on underwater explosion modelling since this agreed with the target of the reference developing project. However, the good results obtained encourage the investigation of other possible fields of application of this innovative technique. One of the most promising application seems to be the study of the artificial fractures induced in warm dry rocks in order to create advantageous conditions for geothermal energy production by means of the so called Enhanced Geothermal System [Moia]. In this frame, a preliminary feasibility study has been scheduled with the aim of investigating the effects of pulses generated by high pressure fluid jets or microexplosions in a geological formation, also coupling a local SPH approach with a generalized CFD problem discretization.

Conclusions

An advanced application of the Smoothed Particle Hydrodynamics method for the numerical modeling of underwater explosion problems has been illustrated in this paper.

The basic features of the numerical model adopted to simulate underwater expansion of a HE gas have been illustrated.

The proposed results have shown that the physics of the investigated problems could be simulated with an adequate degree of accuracy for engineering applications; however, it requires some improvement to solve intrinsic criticisms, such as controlling the local particle refinement that could help to enhance the numerical accuracy in those regions where gas rarefaction takes place.

In addition, further applications in geothermal energy production field are under investigation.

ACKNOWLEDGMENT

This work has been financed by the Research Fund for the Italian Electrical System under the Contract Agreement between RSE S.p.A. (previously ERSE) and the Ministry of Economic Development-General Directorate for Energy and Mining Resources stipulated on July 29, 2009 in compliance with the Decree of March 19, 2009

List of Symbols

A	physical field function (scalar or vector)
c_s	speed of sound
D/Dt	material derivative
e	specific internal energy
h	smoothing length
h_0	initial interparticle distance
ΔV	particle volume
m	mass
n	dimension of the physical space
N	neighboring particles
p	pressure
p_0	reference pressure
$r_{ij}=\lvert \mathbf{x}_i-\mathbf{x}_j \rvert$	modulus of the relative distance vector
$\boldsymbol{U}$	detonation wave characteristic velocity
∇r	radial unit vector
$\mathbf{g}$	gravitational acceleration vector
$\mathbf{u}$	velocity vector
$\mathbf{u}_{ij}$	relative velocity vector
$\mathbf{u}_b$	velocity vector of the solid boundary
$\mathbf{x}$	position vector
$\mathbf{x}_{ij}$	relative position vector
dV	elementary volume
α_M, β_M	constants of Monaghan artificial viscosity
δ	Dirac delta function

γ state equation parameter
ε fluid compressibility modulus
φ, ϑ, r spherical coordinates
μ dynamic viscosity
ν cinematic viscosity
Π Monaghan artificial viscosity
ρ density
ρ_G gas density
ρ_0 reference density
θ_P pressure smoothing coefficient
W kernel smoothing function
$d\Omega$ elementary volume of the continuum
Ω spatial domain
Ω_I compact support (or influence domain) of the i-th particle

REFERENCES

Cooper P.W. "Explosives Engineering". Wiley-VCH, 1937.

Di Monaco A., Manenti S., Gallati M., Sibilla S., Agate G., Guandalini R. "SPH model-ing of solid boundaries through a semi-analytic approach". J. Eng Appl. Comp. Fluid Mech. Vol. 5, No. 1, pp. 1–15 (2011).

Gingold R.A., Monaghan J.J. "Smoothed particle hydrodynamics: theory and application to non-spherical stars". Mon Not Roy Astron Soc, 181-375,1977.

Kedrinskii V.K. "Hydrodynamics of explosion – Experiments and models". Springer, 2005.

Li S., Liu W.K. "Meshfree Particle Methods". Springer Ed. 2004.

Liu G.R., Liu M.B. "Smoothed Particle Hydrodynamics - a Meshfree Particle Method". World Scientific Publ. 2007.

Lucy L. "A numerical approach to the fission hypothesis". Astron J., 82-1013, 1977.

Manenti S., Agate G., Di Monaco A., Gallati M., Maffio A., Guandalini R., Sibilla S. "SPH Modeling of Rapid Sediment Scour Induced by Water Flow". 33rd IAHR Cong. Au-gust 9–14 2009 Vancouver, British Columbia (Canada).

Manenti S., Ruol P. "Fluid-Structure Interaction in Design of Offshore Wind Turbines: SPH Modeling of Basic Aspects". Proc. Int. Workshop Handling Exception in Structural Engineering, Nov. 13–14 2008, Sapienza University (Italy) DOI: 10.3267/HE2008.

Manenti S., Sibilla S., Gallati M., Agate G., Guandalini R. "Prediction of Sediment Scouring through SPH". Proc. 5th SPHERIC Int. Workshop June 23-25 Manchester, Uk, pp. 56-60 2010.

Manenti S., Sibilla S., Gallati M., Agate G., Guandalini R. Experimental and Numerical Modeling of the Impulsive Dynamics of an Underwater non-Cohesive Sediment Deposit subjected to a Gaseous Jet. 7th Int. SPHERIC Workshop - Prato, Italy 29-31 May 2012, pp.381-385.

Moia F., Colucci F., Federici P. "Analisi della sismicità indotta dallo sfruttamento geotermico" - Report RSE 13000780 (February 2013) (in Italian).

Monaghan J.J. "Simulating free surface flows with SPH". Jour. Comput. Phys. Vol. 110, 399-406, 1992.

Monaghan J.J. "Smoothed particle hydrodynamics". Ann. Rev. Astronomy and Astrophys-ics, Vol. 30, 543-574, 1992a.

Monaghan, JJ. "Smoothed particle hydrodynamics". Rep. Prog. Phys. 68 1703–1759, (2005) doi:10.1088/0034-4885/68/8/R01.

Morris J.P., Fox P.J., Zhu Y. "Modeling Low Reynolds Number Incompressible Flows Using SPH". J. Comput. Phys. 136, 214–226 (1997).